ELSEVIER Journal of Electron Spectroscopy and Related Phenomena 114–116 (2001) 1005–1011

JOURNAL OF ELECTRON SPECTROSCOPY and Related Phenomena

www.elsevier.nl/locate/elspec

XANES microspectroscopy of biominerals with photoconductive charge compensation

B. Gilbert[a,*], G. Margaritondo[a], S. Douglas[b], K.H. Nealson[b], R.F. Egerton[c], G.F. Rempfer[d], G. De Stasio[e]

[a]*Ecole Polytechnique, Federale de Lausanne, Switzerland*
[b]*Jet Propulsion Laboratory, California Institute of Technology, Pasadena, CA, USA*
[c]*Physics Department, University of Alberta, Edmonton, Canada T6G 2J1*
[d]*Department of Physics, Portland State University, P.O. Box 751, Portland, OR, USA*
[e]*University of Wisconsin, Department of Geology, Madison WI, USA*

Received 8 August 2000; received in revised form 22 September 2000; accepted 3 October 2000

Abstract

Specimen charging under X-ray illumination is a well known phenomenon that can seriously obstruct the analysis of insulating samples. Synchrotron X-PEEM spectromicroscopy can reach a lateral resolution of 20 nm, 1–2 orders of magnitude larger than electron microscopies, but has the added capacity to probe oxidation state through total yield X-ray absorption near edge structure (XANES) spectroscopy. This capability may be compromised, however, if specimen charging restricts electron emission, as was encountered in the study of silicified bacteria from an Icelandic hot spring microbial mat. Bacteria living in an environment containing a high concentration of dissolved silica provide nucleation sites for amorphous silicate precipitation, a process which may lead to the preservation of the cellular structure, i.e. fossilization. TEM studies of bacteria in progressive stages of mineralization showed that mineral formation was initiated in the extracellular sheath, reaching the cell interior after death. Spectromicroscopy at the Si L-edge of sectioned mineralized bacteria encountered major charging difficulties, which were relieved by simultaneously illuminating the specimen with 325 nm HeCd laser light during the analysis. The low energy light excites mobile free electrons below the work function threshold, which can offset surface positive charge. This approach allowed spectroscopy to be performed from microscopic areas, and may be applicable to a wider range of insulating samples.

Keywords: Microchemical analysis; Photoconductivity; Charging; Mineralization; X-ray absorption; Spectromicroscopy

1. Introduction

Environmental and biological specimens often pose problems for high resolution imaging and microchemical analysis, with electron or X-ray based microprobes, due to charge build up [1]. X-ray PhotoElectron Emission spectroMicroscopy (X-PEEM) has few constraints on sample characteris-

*Corresponding author. Present address: University of Wisconsin–Madison, Synchrotron Radiation Centre, 3731 Schneider Drive, Stoughton, WI 53589, USA. Tel.: +1-608-877-2000; fax: +1-608-877-2001.
E-mail address: bgilbert@dpmail.epfl.ch (B. Gilbert).

0368-2048/01/$ – see front matter
PII: S0368-2048(00)00342-X

tics, which is appealing for the analysis of specimens in their environment. The composition and chemistry of a specimen is observed through the acquisition of laterally resolved soft X-ray absorption spectra, imaging the low energy electrons emitted from the surface [2]. In a recent experiment to elucidate the mineral products of novel sulfur reducing bacteria, bacteria and zinc sulfide microparticles air dried on a conducting substrate were easily analyzed [3,4]. The distribution of physiological elements and anti-tumor drugs may be studied in cultured tumor cells [5], or tumor tissue sections 7 μm thick [6], ashed in a UV/ozone plasma to remove carbon and thin the specimen. Similarly, tumor tissue embedded in resin and sectioned 60 nm thick may be analyzed with no ashing, and no observable charging. Remarkably, iron and manganese oxide mineral phases could be mapped at sub-micron resolution on the polished surface of a millimeter thick rock slice [7]. However, the most serious barrier to thorough analysis is charge formation at the surface. For example, dense protein formations (plaques) associated with dementia form impenetrable, positively charged centers within surrounding tissue, defying attempts to acquire X-ray absorption spectra. These examples demonstrate the wide variety of specimens and preparation techniques encountered. They also hint at the idealistic situation, of performing microchemical analysis at the surface of *any* specimen, regardless of its nature or thickness, minimizing the sample preparation steps that risk altering specimen morphology and chemistry.

A simple model of surface charge formation can be made for uniform samples, leading to the expected exponential dynamic behavior after illumination begins, in agreement with experiment [7]. In complex samples, however, local charge formation can affect imaging and spectroscopy in profound and unexpected ways, creating apparent topography and even negative X-ray absorption features. The alleviation of charging by photoconductivity in fixed cells under both UV [8] and X-ray illumination [7] has been demonstrated. Charge compensation has also been observed inducing photoconductivity in semiconductors analyzed by mass spectrometry [9]. There are very few studies in the literature, however, concerning photoconductivity in specific biological or non crystalline substances.

We have analyzed a number of poorly conducting biological and geological specimens with X-PEEM, with simultaneous near-UV laser illumination to stimulate surface photoconductivity. The samples studied were part of ongoing projects in experimental cancer therapy, geomicrobiology and environmental science. The aim was to observe the effectiveness of photoconductivity in alleviating local charge formation in cells, tissue and minerals. The data presented here come principally from a study of the mineralization of filamentous bacteria originating from hot springs in Iceland [10]. The outer sheath surrounding the filament is thought to provide nucleation sites for precipitation of silica (SiO_2) present at high concentration (490 ppm). The growing mineral coat is unwanted by the bacterium, which may shed layers before becoming encased, and finally internally silicified.

It has been assumed that, depending upon the environmental chemistry, the microorganism itself may be preserved, or fossilized, in the final sediment. Interactions such as this between microorganisms and geological processes are thought to have had a very significant impact on many present day rock beds [11]. Furthermore, metal ions, such as iron or uranium, in solution in the vicinity of the organism may also act as nucleation sites, and be trapped in the resulting matrix. Thus biomineralization processes may be important in remediation of contaminated water bodies, locking toxic ions in insoluble precipitates.

The present understanding of the silicification process is based upon electron microscopy analysis coupled with energy dispersive X-ray spectroscopy (EDS) for elemental analysis, and electron diffraction for structural information. Near edge X-ray absorption spectroscopy is sensitive to both electronic and molecular (or cluster) structure, as demonstrated by the ability of Si L-edge absorption spectroscopy to distinguish between four and six coordinated silicate minerals [12]. Hence spectra acquired from mineralized bacterial filaments directly identified the mineral precipitates as amorphous silica, in agreement with the literature. X-ray absorption techniques are additionally very sensitive to the lighter physiological elements, which we hope will allow simultaneous investigations of organism and mineral chemistry.

2. Experimental

Samples of a microbial mat community from an Icelandic hot spring were fixed in aqueous glutaraldehyde and prepared for transmission electron microscopy (TEM) and X-PEEM analysis by sequential dehydration in ethanol/water solutions, transferred to acetone, and embedded in Epon 812 epoxy resin [10]. Ultrasections 60 nm thick were cut and mounted on specimen grids (TEM) or silicon wafer substrates coated with 200 nm gold layer (X-PEEM).

Cyanobacteria *Calothrix* were isolated from a microbial biofilm near Rock Creek in British Columbia and cultured as part of a study into the effects of aqueous alkaline earth metals on cellular growth and morphology. The full sample preparation procedure may be found in Ref. [13]. Ultrathin sections of fixed cyanobacterial filaments were prepared for TEM and X-PEEM as above.

A schematic view of the MEPHISTO spectromicroscope [2] installed on a synchrotron ring is given in Fig. 1. The total yield of electrons emitted from the surface under X-ray illumination is proportional to the X-ray absorption coefficient, and hence an X-ray absorption spectrum is acquired by recording the emitted electron intensity from microscopic areas of the sample as a function of the photon energy. A magnified photoelectron image of the specimen is formed by the electron optics of the spectromicroscope and projected onto a detector, converted into an optical image at a phosphor screen, captured by a video camera linked to a PC and digitized. The Oregon PhotoElectron Microscope (UV–PEM) has a very similar construction, using two laboratory UV sources, an incandescent mercury lamp or an argon ion laser (244 nm, Lexel Laser, CA).

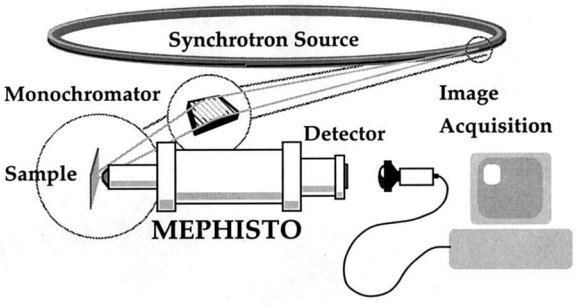

Fig. 1. Experimental set-up for performing spectromicroscopy with MEPHISTO. The essential components are labeled in the diagram and described in the text. The electrostatic lenses which form a magnified, focused electron image of the specimen are located in the body of the spectromicroscope. The synchrotron ring, the monochromator, the sample and the interior of MEPHISTO are all in ultra high vacuum. For photoconductivity trials, a HeCd laser (not shown) illuminated the sample through a UV transmitting sapphire window.

The photoconductivity trials were performed in the MEPHISTO X-PEEM, directing unfocused light at 325 nm (5.4 eV) from a 90 mW cw Helium Cadmium laser (Kimmon, Japan) onto the specimen under simultaneous X-ray illumination. For X-PEEM analysis, the specimen is kept under ultra high vacuum, and hence a sapphire window was used to transmit UV light into the microscope vacuum chamber.

3. Results and discussion

The extent of specimen charging observed in the photoelectron microscope varies substantially with the incident photon energy. This is illustrated in Fig. 2a and b, which show photoelectron micrographs of neighboring ultrathin sections of a cyanobacterial filament embedded in epoxy. Fig. 2a was acquired with X-ray radiation (40 eV), in the MEPHISTO X-PEEM, on the Aladdin storage ring of the UW-Madison Synchrotron Radiation Center. Fig. 2b was acquired with ultra violet radiation (5.4 eV), in the UV–PEM at Portland State University with an argon ion laser. Fig. 2b (UV illumination) correctly shows the sectioned specimen to be flat. By comparison, Fig. 2a (X-ray illumination) shows marked apparent topography around the border of the filament. This is attributed to differences in the electrical conductivity of the epoxy vs. the fixed cyanobacteria. Differential local charging distorts the trajectories of electrons emitted near boundaries, causing the impression of surface relief [7]. This effect is absent with UV illumination, allowing the higher magnification imaging shown in Fig. 2c. The origin of contrast in these images is thus the variation in the ''effective'' work function (work function plus surface potential due to photoelectric charging). Photoconductivity trials with UV laser illumination were not performed on these samples.

A simple explanation of charging behavior as a

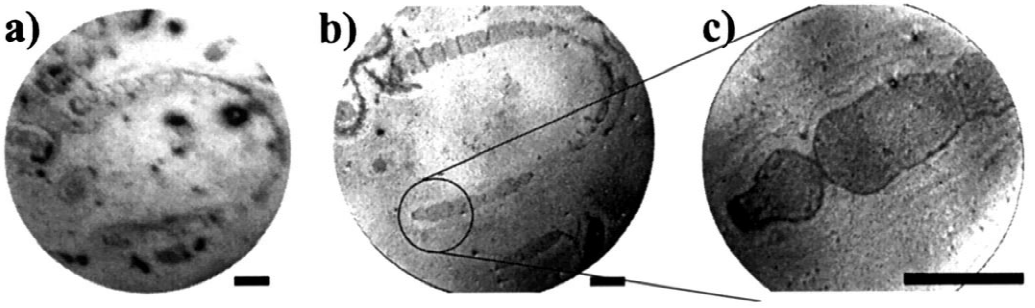

Fig. 2. (a) X-ray photoelectron micrograph of a section of cyanobacterial filament. The apparent topography is an artifact of differential surface charging, which deteriorates image resolution. (b) UV photoelectron micrograph of a subsequent thin section from the same specimen. In the absence of charging, the specimen appears flat, allowing higher magnification imaging. (c) Higher magnification UV photoelectron micrograph of the head region of the filament, clearly showing the outer membrane of the individual bacteria and the layered extracellular sheath. The goal of this and subsequent investigations into problems associated with specimen charging is to be able to combine the higher resolution imaging afforded by UV illumination with the elemental and chemical state information accessible through X-ray spectroscopy. Scale bar=10 μm in each image.

function of photon energy may be obtained by considering only electron excitation and emission at the surface. Fig. 3 displays schematically the secondary electron Energy Distribution Curves (EDCs) anticipated for X-ray and UV illumination of an insulator. At ''high'' photon energies ($h\nu \gg \Phi$, the work function), the secondary electron EDC follows the well-known universal curve depicted in Fig. 3a [14]. Inelastic scattering of primary and Auger electrons travelling in the medium redistributes energy very effectively, and the shape of the EDC is to a good approximation independent of photon energy. As the photon energy is lowered, and approaches the threshold of the photoelectric effect, the mean free paths of primary electrons increases and scattering becomes less significant. The transition between regimes depicted in Fig. 3a and b has not been found in the literature. However, at UV wavelengths, most photoexcited electrons remain within the medium, and hence do not contribute to surface charge formation. At higher photon energies, more electrons have sufficient energy to leave the surface (at least initially, before the formation of a potential barrier). As the photon energy exceeded 100 eV, surface charging decreased, presumably following the reduction in the photoabsorption coefficient (data not shown).

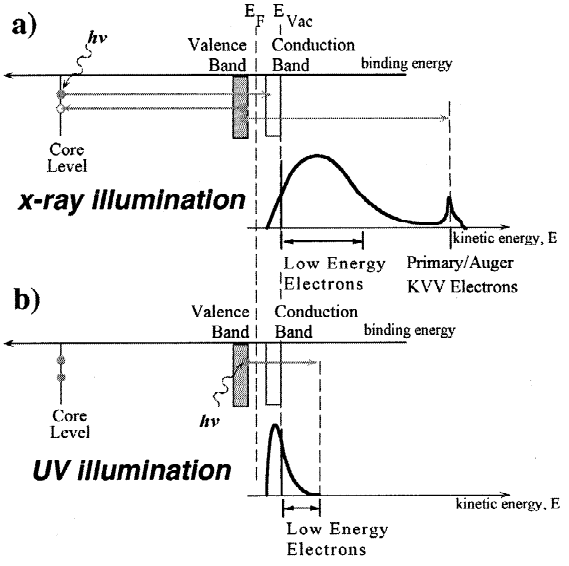

Fig. 3. Schematic energy level diagrams and Energy Distribution Curves (EDCs) for electron emission from an insulating sample illuminated with X-rays (a, top) and UV light (b, bottom). Arrows represent electronic transitions. In each case, the electron shown to leave the specimen without scattering represents the high energy cut-off of the EDC.

Once an insulating specimen is illuminated, the formation of surface charge may be compensated from the specimen mount via a number of routes, including: surface conduction, charge injection, electrical breakdown, and transient photocurrent. The

effectiveness with which photoexcited electrons in the conduction band may redistribute charge depends on the electron/hole mobility and recombination rate, factors which vary enormously across the many organic and inorganic materials present in environmental science specimens. The relatively simple system presented here, silicified bacterial filaments in epoxy resin, showed encouraging signs that internally photoexcited electrons may reduce surface charge formation, and this is qualitatively discussed.

The photoelectron micrograph on the left of Fig. 4 displays a section of bacterial sheath, seen in the visible light micrograph to be highly mineralized, and fractured by the sectioning process. The image taken in the X-PEEM is highly distorted, and all internal details are obscured. The smooth appearance of artificial surface relief is typical of strongly charging samples. This image was acquired with simultaneous X-ray and UV illumination, and clearly the effect of induced photoconductivity on image quality was very limited (the image acquired with no UV illumination is not shown, as the intensity difference is small by eye). Nevertheless, the electron yield from the silicified sheath was elevated in the presence of UV. This is shown in the right image of Fig. 4, which reports the results of a digital subtraction of photoelectron micrographs taken with and without UV laser light. The insulating specimen photoemits more strongly in the presence of UV light. This effect permitted Si L-edge X-ray absorption spectra to be acquired from the specimen, which otherwise was too strongly charged to allow spectroscopy. The spectra acquired with and without UV laser light are given in Fig. 5.

The silicon spectrum matches reference spectra of amorphous silica [12], as expected from the existing electron microscopy data. In addition, the similarity between the lineshape reported, and the lineshapes of analogous compounds, as well as calculated unoccupied density of states, allows the origins of the spectral features to be attributed [15]. In general, near edge absorption features represent transitions to unoccupied electronic levels successively higher in energy, with modulations due to selection rules, as well as multiple scattering phenomena [16]. Thus the absorbing Si occupies a site of tetrahedral symmetry, and the two principal peaks a and b represent respectively Si $2p$ to a_1 (mostly $3s$ character) and Si $2p$ to t_2 (mostly $3p$ character) transitions. The feature labeled c is not associated with silica absorption, although lying at 101 eV could be related to other silicon species, but is unfortunately too weak to allow confident identification. Further technical improvements are necessary before a complete microchemical analysis may be preformed from such a ‘‘difficult’’ specimen.

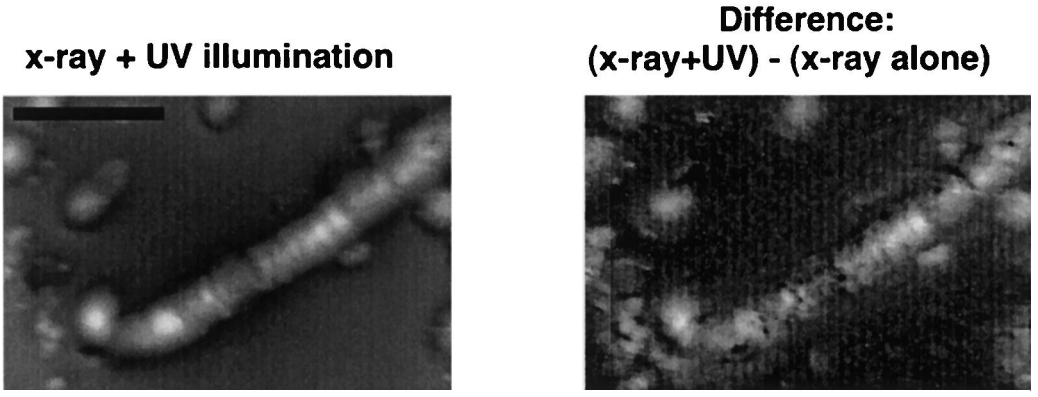

Fig. 4. Photoconductivity enhancement of electron yield. The left image contains a long mineralized bacterial filament, simultaneously illuminated by 90 eV X-rays and 5.4 eV UV laser light. The image resolution is substantially degraded due to charge formation on the silica sheath, obscuring all microstructure within the sheath. The right image is the difference in image intensity on the same specimen, with and without the UV laser light. UV light induced photoconductivity in the mineralized filament is not sufficient to eliminate charging and hence image distortion, but an enhancement in image intensity is evident. Scale bar=10 μm.

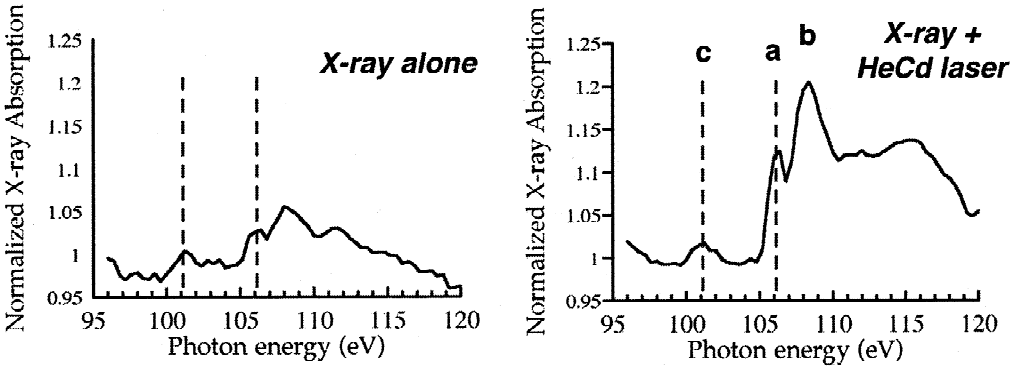

Fig. 5. X-ray absorption microspectroscopy. The spectra shown are from the single mineralized filament of Fig. 4, acquired with and without simultaneous UV illumination. UV induced photoconductivity limits surface charge formation sufficiently to allow silicon L-edge spectra to be recorded. The lineshape of the strong spectrum above 105 eV matches literature spectra from amorphous SiO_2, and features a and b are explained in the text. The feature labeled *c* is not identified. Charging affects spectral resolution as fine structure such as spin–orbit splitting remains obscured.

4. Conclusions

The data show that UV laser illumination was associated with charge compensation on the insulating silicified sheath. The effect was sufficient to perform microspectroscopy, but the image resolution remained very poor. An open question remains: whether the UV illumination stimulated photoconductivity in the silica, or enhanced the conductivity in the surrounding epoxy. It has been observed that charge formation at small specimens of an insulating material (e.g. hollow glass microballs), surrounded by conducting matrices is less severe than analyzing larger areas of the same material. In such cases, the conducting matrix forms a source of free carriers. An alternative method to combat charge problems in X-PEEM analysis might be development of an embedding medium which is itself highly conductive. A related technique such as scanning X-ray fluorescence microanalysis would not be troubled by charge formation, but would also lack sensitivity to the lighter elements. A more detailed analysis would allow the low energy illumination to be tuned to maximize absorption and carrier generation in the specimen or the epoxy, and would situate the UV source within the vacuum chamber to minimize intensity losses. We conclude that photoconductive charge compensation is unlikely to be a universal tool for the spectromicroscopist, capable of rendering any specimen suitable for PEEM analysis. However, it may help to expand the range of X-PEEM farther into new territory.

Acknowledgements

The X-PEEM experiments were performed at the Wisconsin Synchrotron Radiation Center, a facility supported by NSF under grant DMR-95-31009.

References

[1] S. Gunther, A. Kolmakov, J. Kovac, M. Kiskinova, Ultramicroscopy 75 (1998) 35.
[2] G. De Stasio, M. Capozi, G.F. Lorusso, P.-A. Baudat, T.C. Droubay, P. Perfetti, G. Margaritondo, B.P. Tonner, Rev. Sci. Instrum. 69 (1998) 2062.
[3] M. Labrenz, P.L. Bond, B. Gilbert, S.A. Welch, T. Thomsen-Ebert, G. De Stasio, J.F. Banfield, Accepted for publication in Science.
[4] G. De Stasio, B. Gilbert, B.H. Frazer, K.H. Nealson, P.G. Conrad, V. Livi, M. Labrenz, J.F. Banfield, J. Electron Spectrosc. Relat. Phenom. 114–116 (2001) 997.
[5] G. De Stasio, P. Casalbore, B. Gilbert, D. Mercanti, M.T. Ciotti, L.M. Larocca, A. Rinelli, D. Perret, D.W. Mogk, P. Perfetti, R. Pallini, submitted to Proc. Natl. Sci. Am.
[6] B. Gilbert, J. Redondo, P.-A. Baudat, G.F. Lorusso, R. Andres, E.G. Van Meir, J.-F. Brunet, M.-F. Hamou, T. Suda, D. Mercanti, M.T. Ciotti, T.C. Droubay, B.P. Tonner, P. Perfetti, M. Margaritondo, G. De Stasio, J. Phys. D 31 (1998) 2642.

[7] B. Gilbert, R. Andres, P. Perfetti, G. Margaritondo, G. Rempfer, G. De Stasio, Ultramicroscopy 83 (2000) 129.
[8] D.L. Habliston, K.K. Hedberg, G.B. Birrel, G.F. Rempfer, O.H. Griffith, Biophys. J. 69 (1995) 1615.
[9] S. Hayashi, Y. Hashiguchi, J. Vac. Sci. Technol. A 11 (1993) 2610.
[10] S. Schultze-Lam, F.G. Ferris, K.O. Konhauser, R.G. Wiese, Can. J. Earth Sci. 32 (1995) 2021.
[11] S. Schultze-Lam, D. Fortin, B.S. Davis, T.J. Beveridge, Chemical Geology 132 (1996) 171.
[12] D. Li, G.M. Bancroft, M. Kasrai, M.E. Fleet, R.A. Secco, X.H. Feng, K.H. Tan, B.X. Yang, Am. Mineralogist 79 (1994) 622.
[13] S. Douglas, Can. J. Microbiol. 44 (1998) 128.
[14] B.L. Henke, J. Leisegang, S.D. Smith, Phys. Rev. B 19 (1979) 3004.
[15] I. Davoli, E. Paris, S. Stizza, M. Benfatto, M. Fanfoni, A. Gargano, A. Bianconi, F. Seifert, Phys. Chem. Minerals 19 (1992) 171.
[16] P.J. Durham, Theory of XANES, in: Koningsberger and Prins (Eds.), X-ray Absorption: Principles, Applications, Techniques of EXAFS, SEXAFS and XANES, Wiley, New York, 1988, p. 53.